

© 2019 Universidad Nacional Autónoma de México, Facultad de Estudios Superiores Zaragoza.

This is an Open Access article under the CC BY-NC-ND license (<http://creativecommons.org/licenses/by-nc-nd/4.0/>).

TIP Revista Especializada en Ciencias Químico-Biológicas, 22: 1-10, 2019.

DOI: [10.22201/fesz.23958723e.2019.0.172](https://doi.org/10.22201/fesz.23958723e.2019.0.172)

***Proteus mirabilis* expressing Plasmid-encoded toxin (Pet) causes urinary tract alterations**

**Violeta K. Espinosa-Antúnez^{1,2}, Laura E. Castrillón-Rivera², María E. Vega-Memije³,
María Teresa Valenzuela-Vargas⁴, Teresita Sainz-Espuñes², Julieta Luna-Herrera^{5*}
and Jorge I. Castañeda-Sánchez^{2*}**

¹Doctorado en Ciencias Biológicas y de la Salud. Universidad Autónoma Metropolitana- Xochimilco, Mexico City, Mexico. ²Departamento de Sistemas Biológicos. Universidad Autónoma Metropolitana-Xochimilco, Mexico City, Mexico. ³Hospital General “Manuel GEA González” Servicio de Dermatología, Secretaría de Salud de la Ciudad de México, Mexico City, Mexico. ⁴Departamento de Morfología. Escuela Nacional de Ciencias Biológicas, Instituto Politécnico Nacional, Mexico City, Mexico. ⁵Departamento de Inmunología. Escuela Nacional de Ciencias Biológicas, Instituto Politécnico Nacional, Mexico City, Mexico. Calzada del Hueso # 1100, Col. Villa Quietud. Coyoacan 04960, Mexico City, Mexico. E-mails: ^{2*}jcastanedas@correo.xoc.uam.mx, ^{5*}julietalunah@hotmail.com

ABSTRACT

The plasmid-encoded toxin (Pet) is one of the most studied Enterobacteriaceae autotransporters produced by the enteroaggregative *Escherichia coli* (EAEC). It is responsible of morphological changes in enterocytes during EAEC infection. Recently, Pet was found in the genome of the *Proteus mirabilis* RTX339 strain [*P. mirabilis* (Pet+)]. *P. mirabilis* causes complicated urinary tract infections (UTI) in patients having urinary catheters and structural or functional abnormalities. In this study, an UTI was induced in BALB/c female mice with the *P. mirabilis* (Pet+) strain. Mice infected by *P. mirabilis* (Pet+) showed bacterial colonization in bladder and kidney, from the second up to the tenth day post-infection. Morphological changes were evidenced by histology. Multiple exfoliated rounded cells were observed in the bladder transitional epithelium, as well as, structural cell alterations in the kidney cortex. The presence of Pet into exfoliated and parenchymal cells was confirmed by confocal microscopy. Cytoskeleton alterations were observed in those sites where Pet was detected. Pet expressed by *P. mirabilis* (Pet+) strain, contributes to its pathogenicity, affecting urinary tissues during the course of the infection.

Key words: Pet (Plasmid-encoded toxin), *Proteus mirabilis*, urinary tract infection, cytoskeleton, urinary organs.

Alteraciones en el tracto urinario durante la infección con *Proteus mirabilis* que expresa la toxina codificada en plásmido (Pet)

RESUMEN

La toxina Pet (plasmid-encoded toxin) producida por *Escherichia coli* (EAEC) es uno de los autotransportadores más estudiados en la familia Enterobacteriaceae.

Es responsable de cambios morfológicos en enterocitos durante la infección por EAEC. Recientemente, Pet fue encontrada en el genoma de una cepa de *Proteus mirabilis* RTX339 [*P. mirabilis* (Pet+)]. *P. mirabilis* causa infección en el tracto urinario (ITU) en pacientes que usan catéteres o que presentan anomalías estructurales o funcionales. En este estudio una ITU con *P. mirabilis* (Pet+) fue inducida en ratones hembras BALB/c. Los ratones infectados con *P. mirabilis* (Pet+) muestran una colonización bacteriana en vejiga y riñón desde el segundo hasta el día decimo de la infección. Los cambios morfológicos fueron evidenciados por histología. Se observaron múltiples células exfoliadas del epitelio de transición de la vejiga, así como alteraciones morfológicas en la corteza renal. Se confirmó la presencia de Pet en las células exfoliadas y en las del parénquima por microscopía confocal. Las alteraciones del citoesqueleto fueron observadas en los sitios donde se detectó Pet. La toxina Pet expresada por la cepa de *P. mirabilis* (Pet+) contribuye a la patogenicidad y afecta tejidos urinarios durante el curso de la infección.

Palabras clave: Pet (Plasmid-encoded toxin), *Proteus mirabilis*, infección del tracto urinario, citoesqueleto, órganos urinarios.

INTRODUCTION

Proteus mirabilis is a mobile dimorphic Gram-negative bacterium member of the Enterobacteriaceae family (Coker, Poore, Li & Mobley, 2000). This microorganism produces urease and varies from a simple vegetative bacillus with few flagella (swimmer cell) to a lengthened cell with multiple flagella (swarmer cell) (Coker, Poore, Li & Mobley, 2000; O'Hara, Branner & Miller, 2000). It is frequently isolated from the gastrointestinal tracts of humans and animals (Hoeninger, 1964). *P. mirabilis* causes complicated urinary tract infections (UTI), mainly in patients having urinary catheters for prolonged periods or in those with structural or functional abnormalities of the urinary tract (Mobley & Belas, 1995). Some of the most frequent urinary pathologies caused by *P. mirabilis* are: acute pyelonephritis, chronic inflammation, periurethral abscesses, bacteremia, urolithiasis and prostatitis (Allison, Coleman, Jones & Hughes, 1992). UTI caused by *P. mirabilis* involves the expression of virulence factors, as adherence, motility and evasion of the host immune response, which promote bladder and kidney colonization during infection (Coker, Poore, Li & Mobley, 2000; Armbruster & Mobley, 2012).

In the last two decades, new virulence proteins known as autotransporters have been reported mainly in Gram-negative bacteria (Alamuri & Mobley, 2008). These proteins use the type V secretion system to export bacterial components from cytosol to the extracellular milieu (Henderson, Navarro-García, Desvaux, Fernandez & Ala'Aldeen, 2004). Plasmid-encoded toxin (Pet) was first described in enteroaggregative *E. coli* 042 (EAEC) strain (Eslava *et al.*, 1998). It is a secretory protein (104 kDa) that damages the intestinal mucosa causing: I) exfoliation of epithelial cells (enterocytes), II) increase of mucous production and III) abscess development in the cell crypts (Navarro-García *et al.*, 1998). Pet mediated proteolysis breaks the scaffolding protein α -fodrin, inducing contraction of the cytoskeleton, loss of actin stress fibers and loss of the focal contact of cells, which leads to morphological changes like cell rounding and detachment (Canizalez-Roman & Navarro-García, 2003; Navarro-García, Sonnested & Tetter, 2010; Capello *et al.*, 2011). Pet in *P. mirabilis* had not been described until Gutiérrez *et al.* (2012), showed its presence in a clinical isolate denominated as *Proteus mirabilis* RTX339. Pet was found in the culture supernatant and showed high homology with Pet of EAEC 042 (Gutiérrez-Lucas *et al.*, 2012).

The morphological changes of intestinal cells due to Pet from EAEC have been widely studied in several cell lines and in the ligated loops of intestine model (Navarro-García *et al.*, 1998; Navarro-García, Sears, Eslava, Cravioto & Nataro, 1999; Navarro-García, Sonnested & Tetter, 2010; Canizalez-Roman & Navarro-García, 2003; Capello *et al.*, 2011; Henderson *et al.*, 1999; Villaseca *et al.* 2000; Betancourt-Sánchez & Navarro-García, 2009; Sainz *et al.*, 2002; Sui, Dutta & Nataro, 2003;

Rocha-Ramírez *et al.*, 2016). However, there are not studies on the effect of Pet produced by *P. mirabilis* (Pet+) during UTI. Therefore, the aim of this study was to develop an UTI in a mouse model using the *P. mirabilis* (Pet+) strain and to analyze the cellular and morphological changes in relevant urinary organs.

MATERIALS AND METHODS

Mouse strain

Female BALB/c mice, 6 weeks old weighing 17-20 g, were obtained from the Unidad de Experimentación y Producción de Animales de Laboratorio (UPEAL), at the Universidad Autónoma Metropolitana-Xochimilco. All animals were kept at 21-24°C in a 12h light/dark cycle. They were fed with Purina® and pathogen-free purified water ad libitum. Mice were handled in accordance with the international and Mexican standards for animal protection (DOF, 2002).

Bacterial strains

The *P. mirabilis* RTX339 strain was isolated from a patient and was characterized for secreting Pet (Gutiérrez-Lucas *et al.*, 2012). *P. mirabilis* RTX267 and the EAEC 042 were also clinical isolates, the first was a non-secreting Pet isolate, and the last was an enteroaggregative *E. coli* isolate, characterized for secreting Pet (Nataro *et al.*, 1995). All the strains were cultivated in Luria broth, at 37°C overnight.

Detection of pet by PCR analysis

DNA from *P. mirabilis* RTX339, EAEC 042 and *P. mirabilis* RTX267 strains was extracted using the wizard DNA purification kit (Promega) following the manufacturer's instructions. PCR was carried out using a PCR QIAGEN kit (QIAGEN). The PCR for *pet* detection was performed as previously described using the primers U250F (forward) 5'-TGACTCTGCATGGATTGAGC-3' and U250R (reverse) 5'-GACGCATCACTCAGTACAGT-3' (Gutiérrez *et al.*, 2012).

Pet detection by Western blot assay

Bacterial secreted proteins were recovered from Luria broth supernatants, which were inoculated with each of the strains at 37°C overnight. Cell cultures were centrifuged at 9,000 × g for 15 minutes. The supernatant was precipitated with ammonium sulfate at 60% of saturation and kept overnight at 4°C. Then, samples were centrifuged at 12000 × g for 45 minutes, re-suspended in PBS and dialyzed using a nitrocellulose membrane (Spectra/Por® molecular porous membrane tubing MWCO: 12,000-14,000). Finally, the dialyzed proteins were centrifuged at 24,600 × g for 15 min and the supernatants stored at -20°C until use (Gutiérrez *et al.*, 2012). A concentration of 100 mg from each of the protein samples were subjected to SDS-PAGE electrophoresis (12% gel) as described by Laemmli (1970). Protein bands were stained with Coomassie blue R-250 (BioRad). Proteins were transferred to PVDF membranes (Millipore) for Western blot analysis as described by Towbin *et*

al. (1979) (Towbin, Staehelin & Gordon, 1979). One membrane was incubated with a rabbit anti-*P. mirabilis*-Pet antibody using a 1:256 dilution, while the other was incubated with a rabbit anti-EAEC 042-Pet antibody according to Gutiérrez *et al.* (2012). Latter, a goat anti-rabbit IgG coupled to horseradish peroxidase (HRP) (Thermo Scientific), was used at a 1:5,000 dilution. Reaction was detected with a DAB kit (Dako®).

Urinary tract infection

Five mice were employed in each group viz., *P. mirabilis* (Pet+), EAEC 042 (Pet+), *P. mirabilis* (Pet-) and a control group remained uninfected (inoculated only with PBS). Mice were anesthetized with ketamine [60mg/Kg] and xilazine [10mg/Kg], and transurethral inoculated with 50 μ L of the corresponding bacterial suspension containing approximately 5×10^7 CFU (Reis *et al.*, 2011; Hung, Dodson & Hultgren, 2009).

Bacterial CFU determination during infection

Urine and urinary organs were collected under sterile conditions at 2, 4, 7 and 10 days post-infection. The urinary organs were homogenized with 1mL of sterile PBS. Subsequently, 100 μ L of serial dilutions of organ-homogenates and urine were spread on MacConkey agar and incubated at 37 °C for 24 hours. The colony count was recorded and the CFU/mL for the urine samples and CFU/g tissue for the urinary organs were determined. Graphs and statistical analyses (Student's t-test) were performed using the GraphPad Prism 6 software.

Histopathological evaluation of urinary tissues

Histological sections were prepared as follows: bladder and kidney of each experimental group were recovered in sterile conditions at day 7 post-infection; organs were fixed with 10%

paraformaldehyde and embedded in paraffin. Serial sections of approximately 5 μ m were sliced and placed on glass slides. Preparations were stained with hematoxylin and eosin according to the procedures of the Biological Stain Commission manual (Clark, 1981). Cellular structures and morphological alterations were observed at 100X, 400X and 1000X magnifications in an optical microscope (Carl Zeiss).

Detection of Pet in urinary organs by confocal microscopy

Histological sections of each group were de-paraffinized and then permeabilized for 10 minutes with 0.2% triton X-100 at room temperature. Actin was stained with rhodamine-phalloidin (100 ng/slide) (Santa Cruz Biotechnology, USA.) for 30 minutes. Later, the slides were blocked with 4% albumin for 30 minutes. Pet was labeled with rabbit anti-Pet antibody diluted 1:100 and left overnight at 4°C, then stained with a fluorescein isothiocyanate (FITC) labeled goat anti-rabbit immunoglobulin G (IgG) (Santa Cruz Biotechnology) at 1:300 dilution for 2 hours at room temperature. Slides were mounted with vectashield® and observed in a LSM 510 Carl Zeiss confocal microscope at 63X magnifications and analyzed by LSM5 Pascal Zeiss software.

RESULTS

Pet detection in *P. mirabilis* (Pet+)

The presence of Pet in *P. mirabilis* RTX339 was ascertained by genotypic and phenotypic approaches. The PCR results showed an amplicon of 250 pb as expected for *P. mirabilis* RTX339 (Pet+) and for EAEC 042, no amplification was detected for *P. mirabilis* RTX267 strain (Figure 1a). At the level of protein detection, the results showed the presence of a protein of approximately 104 kDa in both *P. mirabilis* RTX339 and EAEC 042 samples (Figure 1b), and *P. mirabilis* RTX267 did

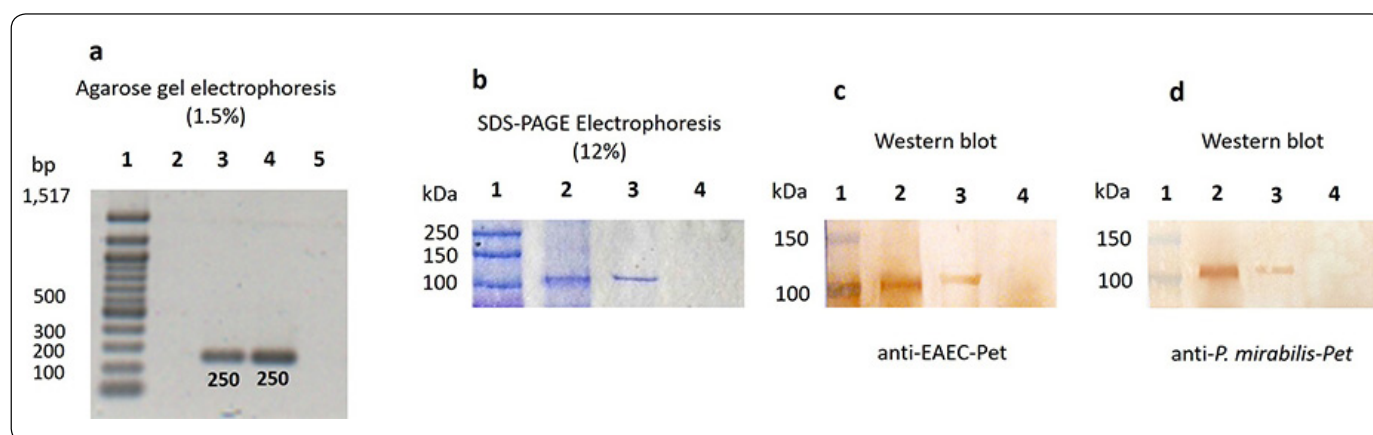


Figure 1. Pet detection in *P. mirabilis* (Pet+). (a) DNA of each microorganism was analyzed by PCR using specific primers for Pet, the agarose electrophoresis presents a 250 pb amplicon for *P. mirabilis* RTX339 and EAEC 042. Line 1, pb-marker; line 2, negative control (water + all PCR components); line 3, *P. mirabilis* RTX339 DNA; line 4, EAEC 042 DNA; line 5, *P. mirabilis* RTX267 DNA. (b) SDS-PAGE-Coomassie blue stained shows a protein band of approximately 104 kDa in both *P. mirabilis* RTX339 (line 2) and EAEC 042 (line 3) samples; no band of 104 kDa was detected for *P. mirabilis* RTX267 (line 4). (c) Western Blot assay using anti-Pet antibody from EAEC 042; line 1, molecular weight marker (MWM); line 2, *P. mirabilis* RTX339; line 3, EAEC 042; lane 4, *P. mirabilis* RTX267 and (d) Western Blot assay using anti-Pet antibody from *P. mirabilis* RTX339.

not expressed any protein of this molecular weight. Beside, Pet identity was confirmed by Western blot using rabbit anti-Pet antibodies raised with *P. mirabilis* RTX339 (Pet+) (Figure 1c) or with EAEC 042 (Figure 1d).

Colony forming units (CFU) in urine and urinary organs during infection

Colony-forming unit counts in urine and urinary organs of mice infected with *P. mirabilis* RTX339, EAEC 042 and *P. mirabilis* RTX267 were carried out at 2, 4, 7 and 10 days post-infection, to determine urinary infection establishment and progress (Figure 2).

The three strains were able to establish a urinary infection after two days post-infection with CFUs higher than 10^4 /mL or /g per tissue, both in the urine samples and in the urinary organs, respectively. Only in the case of EAEC 042 urine samples (Figure 2a), the bacterial counts were lower than 10^4 CFU/ml, but in contrast, bacterial counts in bladder and kidney were above 10^4 CFU/ml, indicating an active bacterial infection (Figures 2b and 2c). In general, the highest bacterial counts were recovered from bladder; being particularly higher in *P. mirabilis* RTX339 infection (Figure 2b). All three bacterial infections reached kidneys with EAEC 042 presenting the

highest bacterial numbers (Figure 2c). By day 10 post-infection a significant decrease of the CFU in each of the samples was observed (Figure 2), but a complete bacterial elimination was not accomplished.

Histopathological evaluation of bladder and kidney of mice infected with different bacterial strains

Histological analysis of tissue samples from mouse urinary organs infected with each strain, showed loss of cellular integrity, exfoliation, necrosis and hemorrhage compared to urinary organs inoculated only with vehicle.

Healthy mouse bladders (Figure 3a), showed cellular structures without morphological alterations. The transitional epithelium (TE), of the mucosa comprising 4 to 6 cuboid cellular layers, was found broadly attached to each other. In contrast, the bladders of mice infected with *P. mirabilis* RTX339 (Pet +) showed the presence of exfoliated cells belonging to transitional epithelium that were rounded (ERC) and detached: in addition, elongated cells were also observed on this layer. In the lamina propria (LP), cellular and extracellular matrix damage was seen (Figure 3b). Bladders of mice infected with EAEC 042 presented similar morphological alterations to *P. mirabilis* RTX339 although with greater intensity (Figure 3c). The transitional epithelium of the

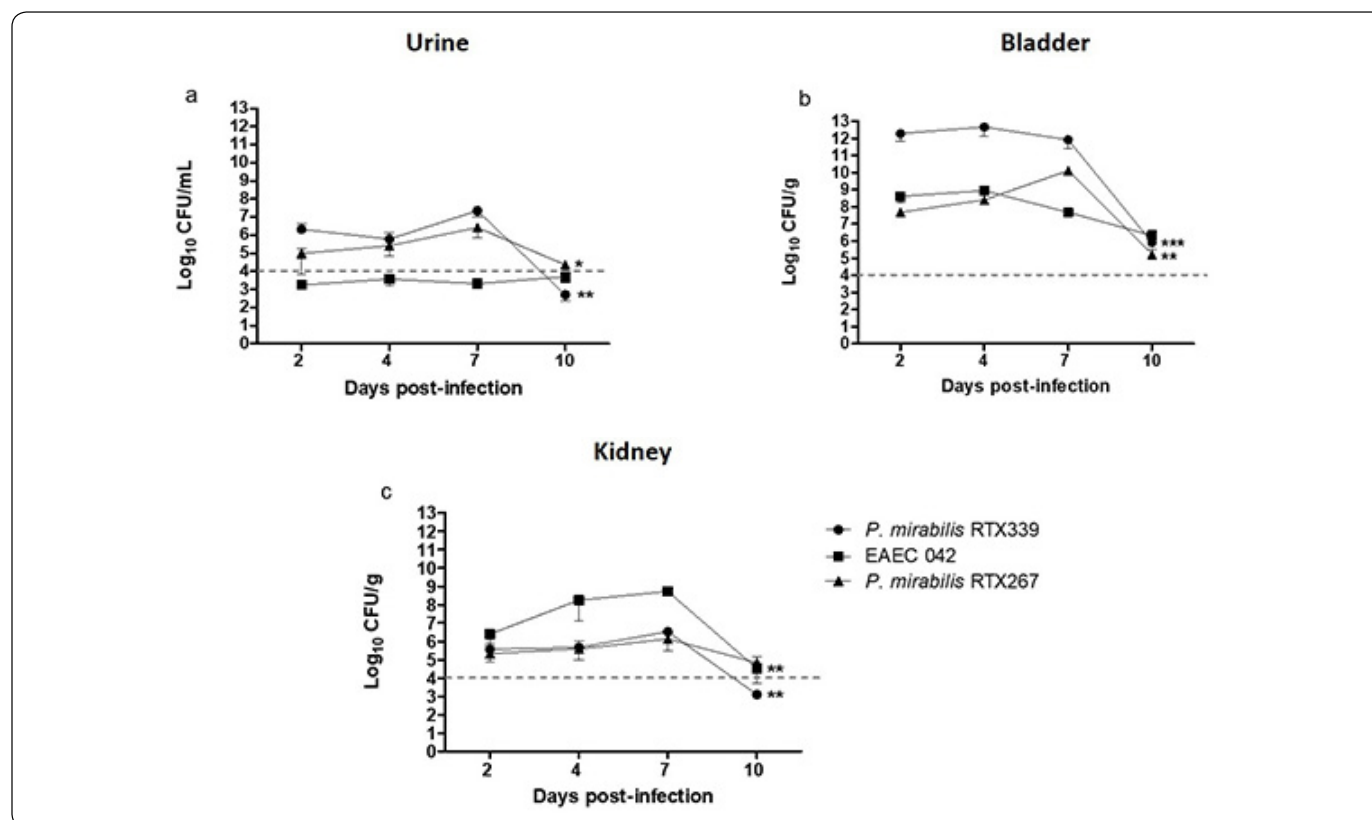


Figure 2. Colony forming units (CFU) in urine and urinary organs during infection. Colony-forming unit counts in urine (a), bladder (b) and kidney (c) of mice infected with *P. mirabilis* RTX339, *P. mirabilis* RTX267 and EAEC 042. Evaluation at 2, 4, 7 and 10 days post-infection. $p < 0.05$: * $p=0.01$, ** $p=0.001$, *** $p=0.0001$.

bladders of mice infected with *P. mirabilis* RTX267 (Figure 3d) showed changes in the form of the cellular structures with ruffling shapes, but without cellular loss in the layer.

Regarding to the analysis of kidney tissues of healthy mice, showed characteristic cellular structures like: I) glomerular cells surrounded by the Bowman's capsule and II) proximal tubules displaying uniform cuboidal cells structures firmly connected to each other (Figure 4a). In contrast, kidney tissues of mice infected with *P. mirabilis* RTX339 (Pet+) (Figure 4b) and EAEC 042 (Pet+) (Figure 4c), showed similar histological alterations as: I) presence of exfoliated rounded cells around arteries, II) loss of proximal tubules close to glomeruli, III) loss of cuboidal cellular structures of tubules, IV) loss of crest structure and bigger size of the glomeruli and V) presences of erythrocytes between the tubules. However, kidney's tissue of mice infected with EAEC 042 presented more severe morphological changes than those infected with *P. mirabilis* RTX339 (Pet+). On the other hand, tissues of mice infected with *P. mirabilis* RTX267 (Pet-) presented: I) dilatation of proximal convolute tubules

with loss of their epithelial lining, II) loss of crest structure and bigger size in glomeruli and III) absence of exfoliated cells around arteries (Figure 4d).

In situ Pet detection in urinary infected tissues

An immunofluorescence assay was carried out in urinary tissues to detect *in situ* the presence of Pet during *P. mirabilis* (Pet+) infection (Figures 5 and 6). No exfoliated rounded cells, nor the presence of Pet signal were observed in bladder tissues of healthy mice (Figure 5a). The analysis of bladder tissues of mice infected with *P. mirabilis* (Pet+) (Figure 5b) and EAEC 042 (Pet+) (Figure 5c) showed the presence of Pet inside exfoliated rounded cells; at the same time, these rounded cells showed actin reorganization. No exfoliated rounded cells, nor the presence of Pet signal were observed in bladder tissues of mice infected with *P. mirabilis* (Pet-) (Figure 5d).

Pet was absent in the histological samples of healthy mice (Figure 6a). Regarding the analysis of kidney tissues, Pet was lesser extent in the *P. mirabilis* RTX339 infected kidney tissues

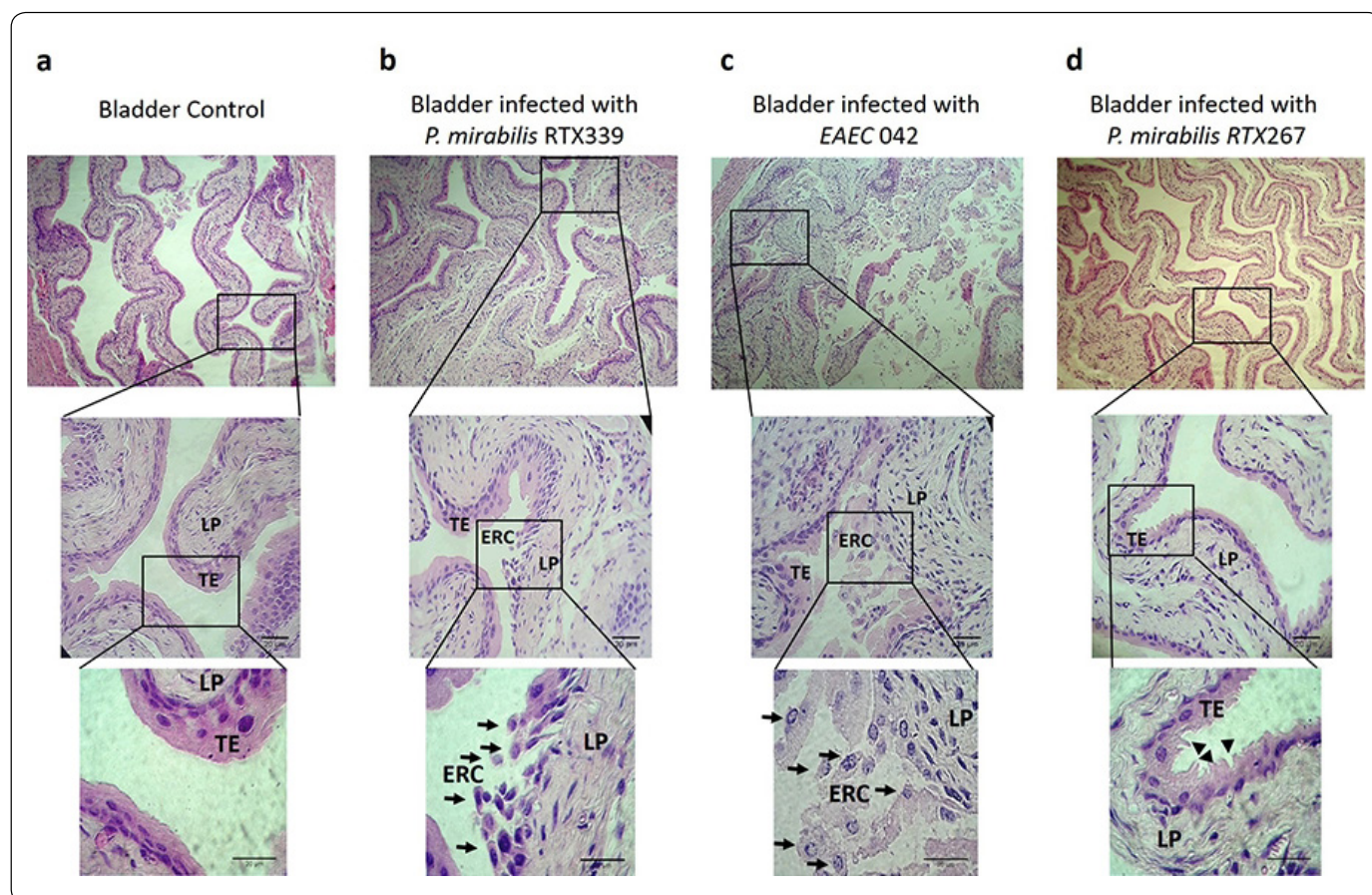


Figure 3. Histopathological evaluation of bladder tissues infected with different bacterial strains. a) Bladder tissue of mice inoculated with PBS. b) Bladder tissue of mice infected with *P. mirabilis* RTX339 (Pet+). c) Bladder tissue of mice infected with EAEC 042 (Pet+). d) Bladder tissue of mice infected with *P. mirabilis* (Pet-). Histological sections were stained with hematoxylin and eosin. Arrows show the presence of exfoliated rounded cells from transitional epithelium. Arrowheads show the ruffling membrane of transitional epithelium. Bar= 20µm. TE: Transitional epithelium, ERC: Exfoliated rounded cells and LP: Lamina propria.

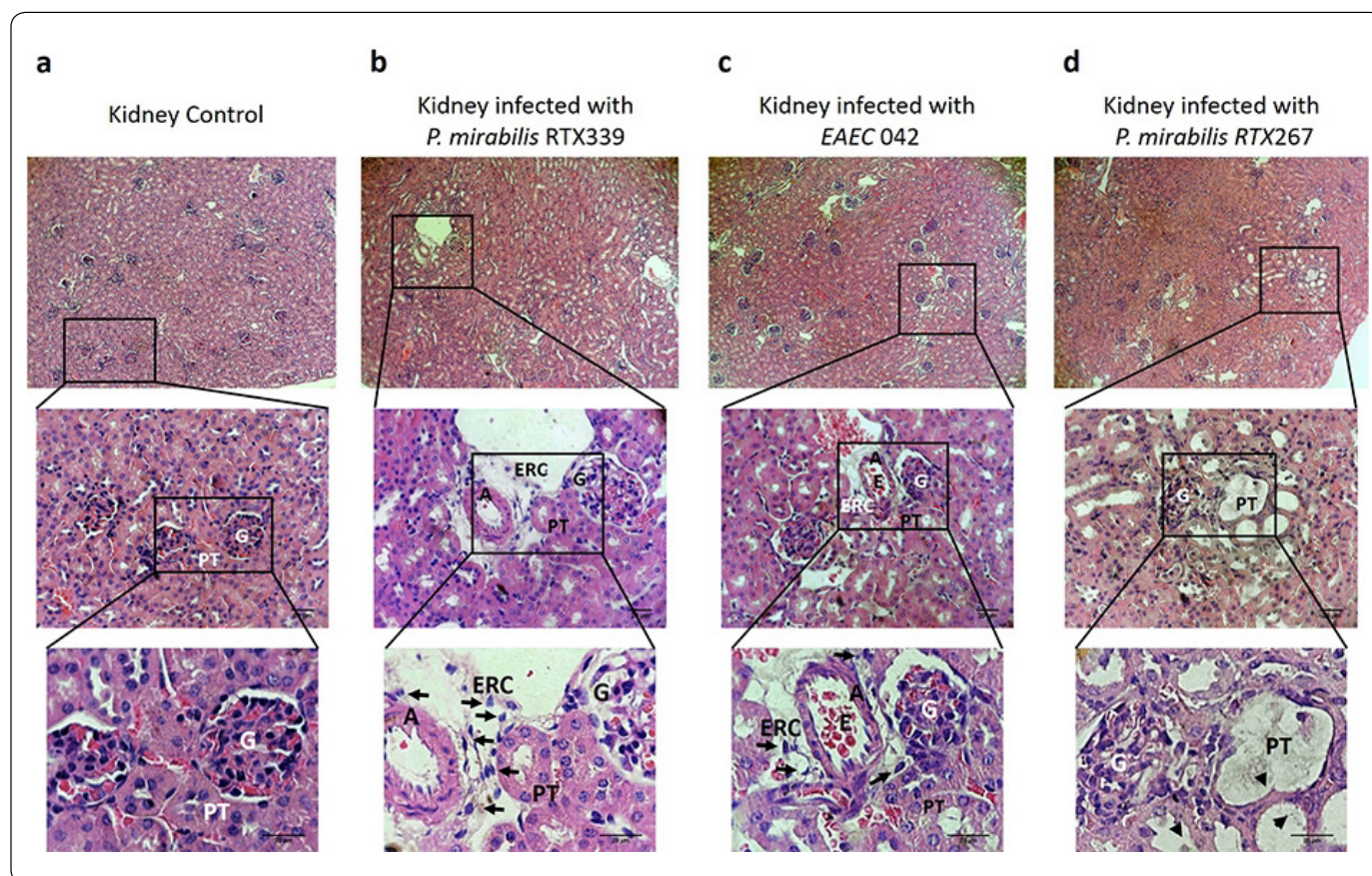


Figure 4. Histopathological evaluation of kidney tissues of mice infected with different bacterial strains. a) Kidney tissue of mice inoculated with PBS, b) kidney tissue of mice infected with *P. mirabilis* RTX339 (Pet+), c) kidney tissue of mice infected with EAEC 042 (Pet+), d) kidney tissue of mice infected with *P. mirabilis* RTX267 (Pet-). Histological sections were stained with hematoxylin and eosin. Arrows show the presence of exfoliated rounded cells around the arteries. Arrowheads show dilatation of the proximal convoluted tubules. Bar= 20 μ m. G: Glomerulus, PT: Proximal tubule, ERC: Exfoliated rounded cells, A: Artery and E: Erythrocytes.

(Figure 6b) and highly expressed in kidneys of mice infected with EAEC 042 (Figure 6c). In the EAEC 042 infected tissue Pet was observed in many structures like proximal tubules, arteries and glomeruli. In the glomeruli Pet was observed in the endothelial cells. All these structures presented beside Pet, morphological changes and cytoskeleton reorganization. Tissues from kidneys infected with *P. mirabilis* RTX339 had similar alterations but in lower extent. Pet was absent in samples of mice infected with *P. mirabilis* RTX267 (Pet-) (Figure 6d).

DISCUSSION

Urinary tract infection (UTI) caused by *P. mirabilis* is the result of a complex interaction between the pathogen and the host. During infection, the pathogen expresses numerous virulence factors, which appear to be essential for the development and during the course of infection (Coker, Poore, Li & Mobley, 2000). Pet is a member of autotransporter class of secreted proteins (Eslava *et al.*, 1998), which belongs to the serine protease autotransporters of Enterobacteriaceae (SPATE), many SPATE have been characterized as important virulence factors for

the Enterobacteriaceae family (Henderson, Navarro-Garcia, Desvaux, Fernandez & Ala'Aldeen, 2004). In this study, we describe the presence of Pet and the morphological changes in murine urinary tissues during the course of an infection with *P. mirabilis* (Pet+).

Pet was described and studied for the first time as a cytotoxic protein produced by EAEC 042 (Eslava *et al.*, 1998). A recent study of an atypical enteropathogenic *E. coli* clinical isolate also showed the expression of Pet (Ruiz *et al.*, 2014). In this study, we corroborate the presence of Pet in *P. mirabilis* RTX339 (Pet+) strain through genotypic and phenotypic assays, as previously demonstrated by Gutiérrez *et al.*, (2012). Pet is not normally present in *P. mirabilis*, so, it is possible that *pet* was acquired by *P. mirabilis* RTX339 by horizontal gene transfer from an EAEC (Pet+) strain. Pet is encoded in the virulence plasmid (PAA) in EAEC and is a mobile unit that favors horizontal gene transfer processes. The process of how *P. mirabilis* (Pet+) acquired *pet* and how it was incorporated into the bacterial chromosome, are issues that have to be elucidated.

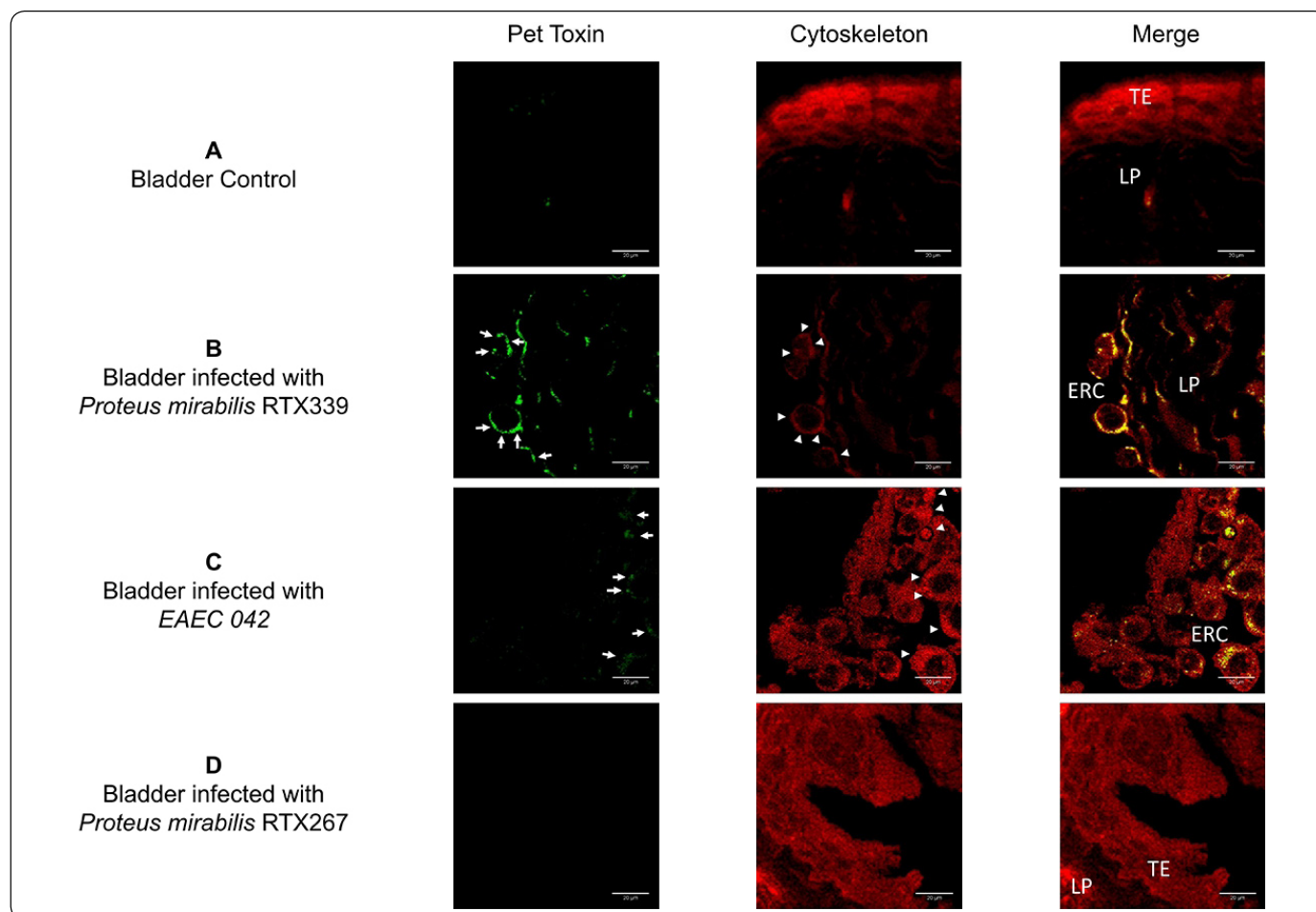


Figure 5. Detection of Pet in bladder tissue infected with different bacterial strains. a) Bladder tissue of mice inoculated with PBS, b) bladder tissue of mice infected with *P. mirabilis* RXT339 (Pet+), c) bladder tissue of mice infected with EAEC 042 (Pet+), d) bladder tissue of mice infected with *P. mirabilis* RTX267 (Pet-). Arrows show the presence of Pet. Arrowheads show the presence of actin aggregates. Bar = 20µm. TE: Transitional epithelium, ERC: Exfoliated rounded cells and LP: Lamina propria.

To observe the characteristics of the host - *P. mirabilis* (Pet+) interaction, in this study we first developed an experimental murine UTI with *P. mirabilis* Pet+ clinical isolates. Both strains of *P. mirabilis* (Pet+ and Pet-) used in the study were isolated from human urine from several UTI occurring simultaneously in a hospital facility; one of them was reported to causes a severe UTI (Gutiérrez-Lucas *et al.*, 2012). EAEC 042 strain in our study was employed because this strain is characterized for secreting Pet. Several reports have demonstrated that EAEC strains may develop UTI (Olesen *et al.*, 2012; Herzog *et al.*, 2014). Also, previous studies showed that in order to establish an UTI (bladder colonization) in murine models, over than 10^4 CFU are required (Hannan, Mysorekar, Hung, Isaacson-Schmid & Hultgren, 2010). In this study could establish a bladder colonization from the second day of infection with the three strains under study, with CFU loads higher than 10^4 , in our model, by the tenth day post-infection a significant decrease of the CFU in urine, bladder or kidney each was observed, without a complete bacterial eradication (Figure 2).

Many *in vitro* and *in vivo* assays have been performed to understand the mechanism of action of Pet from EAEC 042. Pet induces cytotoxic and cytopathic effects on different cell lines, in rat ileal loop and in the intestine of mice infected with EAEC 042, modifying the morphological conformation of enterocytes from cuboidal to a rounded shape, this modification is due to the proteolysis of α -fodrin scaffolding protein of the cytoskeleton, resulting in reorganization of actin filaments (Navarro-García *et al.*, 1998; Navarro-García, Sears, Eslava, Cravioto & Nataro, 1999; Navarro-García, Sonnedstet & Tetter, 2010); Canizalez-Roman & Navarro-García, 2003; Capello *et al.*, 2011; Henderson *et al.*, 1999; Villasaca *et al.*, 2000; Betancourt-Sánchez & Navarro-García, 2009; Sainz *et al.*, 2002; Sui, Dutta & Nataro, 2003; Rocha-Ramírez *et al.*, 2016). Previous histological analysis of the ileal loop and the intestine of mice inoculated with purified Pet and EAEC 042 revealed the hypersecretion of mucus and the presence of abundant exfoliated rounded cells belonging to the intestinal mucosa (Navarro-García *et al.*, 1998; Sainz *et al.*, 2002; Rocha-Ramírez

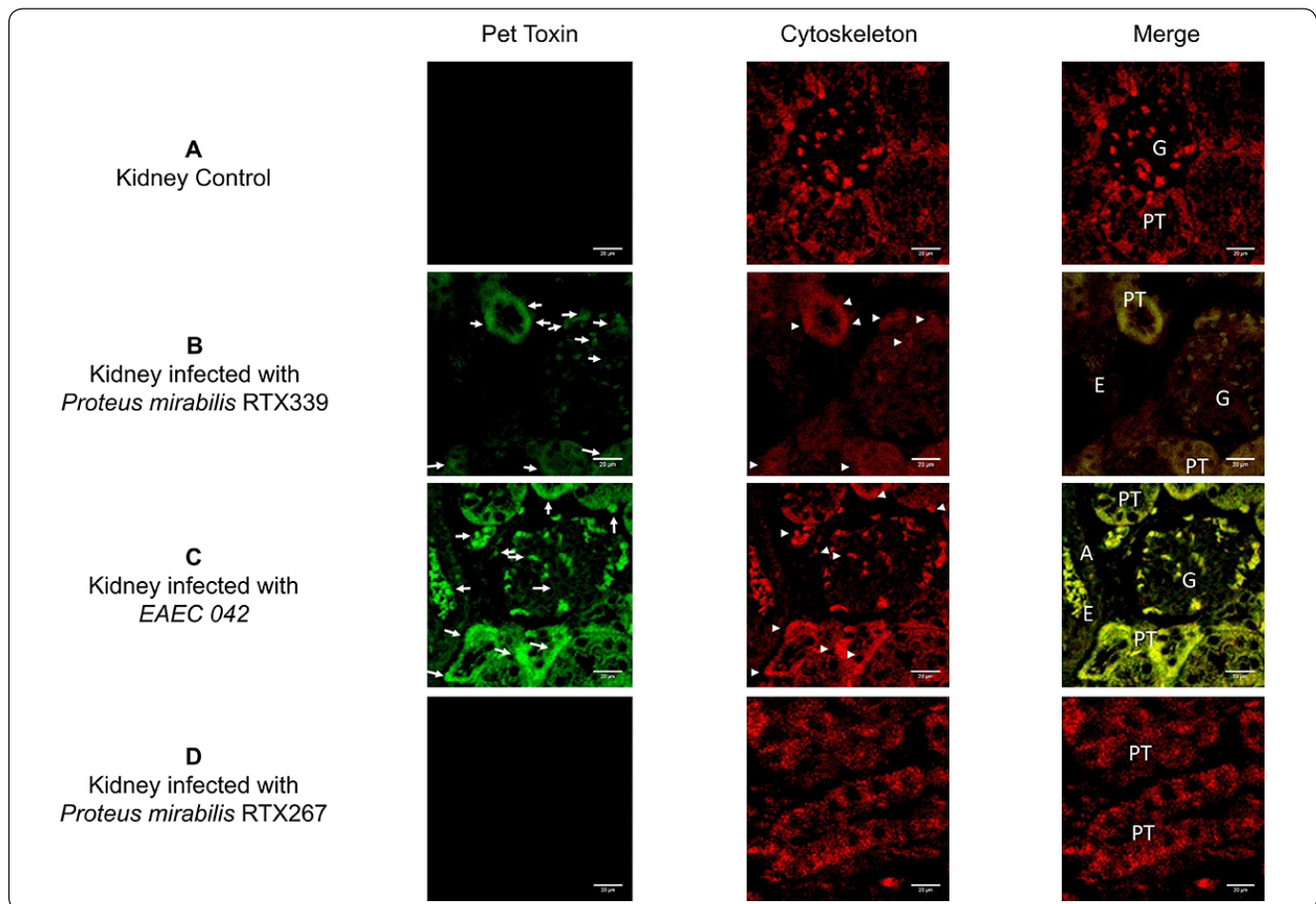


Figure 6. Detection of Pet in kidney tissue of mice infected with different bacterial strains. a) Kidney tissue of mice inoculated with PBS, b) kidney tissue of mice infected with *P. mirabilis* RTX339 (Pet+), c) kidney tissue of mice infected with EAEC 042 (Pet+), d) kidney tissue of mice infected with *P. mirabilis* RTX267 (Pet-). Arrows show the presence of Pet. Arrowheads show the presence of actin aggregates. Bar= 20µm. G: Glomerulus, PT: Proximal tubule, A: Artery and E: Erythrocytes.

et al., 2016). In our study, the histological analysis of urinary tissues of mice infected with *P. mirabilis* (Pet+) and EAEC 042 (Pet+), showed the presence of exfoliated rounded cells, which are in accordance to those exfoliated rounded cells found in the intestinal infection by EAEC 042. Furthermore, we also observed greater degree of damage in urinary tissues of mice infected with EAEC 042 compared to urinary tissues of mice infected with *P. mirabilis* (Pet+). Furthermore, the presences of Pet in those sites with histological alterations, was confirmed by immunofluorescence (Figures 5 and 6). The presence of Pet also correlated to zones with actin reorganization. These results are also in agreement with morphological changes observed in cell lines treated with purified Pet or infected with EAEC 042 (Canizalez-Roman & Navarro-García, 2003; Capello *et al.*, 2011; Navarro-García, Sears, Eslava, Cravioto & Nataro, 1999; Sui, Dutta & Nataro, 2003; Betancourt-Sánchez & Navarro-García, 2009). Furthermore, we observed a greater production of Pet in urinary tissues of mice infected with EAEC 042 in comparison with urinary tissues of mice infected

with *P. mirabilis* (Pet+); these differences could be related to: I) that in case of EAEC 042 *pet* is harbor in a multicopy plasmid (Eslava *et al.*, 1998), in comparison to *P. mirabilis* (Pet+), which harbors a single copy plasmid in the bacterial genome (Gutiérrez-Lucas *et al.*, 2012); and II) differences in adhesion of the pathogen to the urinary epithelium, this feature is important for Pet delivery; in case of EAEC 042 the aggregative adhesion fimbria (AFF) and Pet are harbored in the plasmid PAA, which as was mentioned earlier is present as a multicopy plasmid in EAEC 042 (Eslava *et al.*, 1998), AFF has been correlated with the adhesion to urinary cells in an *in vitro* model of UTI (Boll, Struve, Olesen, Stahlhut & Kroghelt, 2013).

Even though in the present study we could demonstrate morphological alterations and the presences of Pet in urinary tissues infected with *P. mirabilis* (Pet+), additional studies are needed to confirm the mechanism of action of Pet produced by *P. mirabilis* (Pet+) during urinary tract infection and how

adherence factors as mannose resistant *Proteus* like fimbriae, mannose resistant *Klebsiella* fimbriae, Non agglutinating fimbriae also named urothelial cell adhesion, *Proteus mirabilis* fimbriae and ambient temperature fimbriae are correlated to delivery of Pet in host cells.

CONCLUSIONS

This study shows the first evidences of pathological alterations induced in an experimental UTI caused *P. mirabilis* (Pet+), suggesting that this toxin plays an important role in the pathogenesis of *P. mirabilis* (Pet+).

Conflict of interest: The authors declare that they have no conflict of interest.

Ethical approval: All applicable national, and/or institutional guidelines for the care and use of animal were followed.

ACKNOWLEDGMENTS

Violeta K. Espinosa-Antúnez is a Ph.D. student on the *Doctorado en Ciencias Biológicas y de la Salud* at the Universidad Autónoma Metropolitana, Mexico City, Mexico. Supported by grant 14801480 from CONACYT, Mexico.

The authors thank Dra. Sonia López-García for her technical support with fluorescence microscopy assays and Dra. Daniela Salado-Leza for critical and helpful comments of this manuscript.

Jorge I. Castañeda Sánchez and Julieta Luna Herrera are SNI-CONACYT fellows. Jorge I. Castañeda Sánchez, Laura E. Castrillón Rivera are PRODEP-SEP profile professors. Julieta Luna Herrera is a COFAA and EDI fellow from the Instituto Politécnico Nacional. María Teresa Valenzuela Vargas is a COFAA and EDD fellow from the Instituto Politécnico Nacional.

REFERENCES

- Alamuri, P. & Mobley, H.L.T. (2008). A novel autotransporter of uropathogenic *Proteus mirabilis* is both a cytotoxin and an agglutinin. *Mol. Microbiol.*, **68**(4), 997-1017. DOI: 10.1111/j.1365-2958.2008.06199.x
- Allison, C., Coleman, N., Jones, P.L. & Hughes, C. (1992). Ability of *Proteus mirabilis* to invade human urothelial cells is coupled to motility and swarming differentiation. *Infect. Immun.*, **60**(12), 4740-4746.
- Armbruster, C.E. & Mobley, H.L.T. (2012). Merging mythology and morphology: the multifaceted lifestyle of *Proteus mirabilis*. *Nat. Rev. Microb.*, **10**, 473-754. DOI: 10.1038/nrmicro2890
- Betancourt-Sánchez, M. & Navarro-García, F. (2009). Pet secretion, internalization and induction of cell death during infection of epithelial cells by enteroaggregative *Escherichia coli*. *Microbiol.*, **155**(9), 2895-2906. DOI: 10.1099/mic.0.029116-0
- Boll, E.J., Struve, C., Boisen, N., Olesen, B., Stahlhut, S.G. & Krogfelt, K.A. (2013). Role of enteroaggregative *Escherichia coli* virulence factors in uropathogenesis. *Infect. Immun.*, **81**(4), 1164-1171. DOI: 10.1128/IAI.01376-12
- Canizalez-Roman, A. & Navarro-García, F. (2003). Fodrin CaM-binding domain cleavage by Pet from enteroaggregative *Escherichia coli* leads to actin cytoskeletal disruption. *Mol. Microbiol.*, **48**(4), 947-958. DOI: 10.1046/j.1365-2958.2003.03492.x
- Cappello, R.E., Estrada-Gutiérrez, G., Irlés, C., Giono-Cerezo, S., Bloch, R.J. & Nataro, J.P. (2011). Effects of the plasmid-encoded toxin of enteroaggregative *Escherichia coli* on focal adhesion complex. *FEMS Immunol. Med. Microbiol.*, **61**(3), 301-314. DOI: 10.1111/j.1574-695X.2010.00776.x
- Clark G. (1981) Staining Procedures Used by the Biological Stain Commission. 4th Edition, Williams & Wilkins, Baltimore, London, 412.
- Coker, C., Poore, C., Li, X. & Mobley, H.L.T. (2000). Pathogenesis of *Proteus mirabilis* urinary tract infection. *Microbes Infect.*, **2**(12), 1497-1505. DOI: 10.1016/S1286-4579(00)01304-6
- Diario Oficial de la Federación de México (2002, 22 agosto). Especificaciones técnicas para la producción, cuidado y uso de los animales de laboratorio. Secretaría de Agricultura, Ganadería, Desarrollo rural, Pesca y Alimentación. Servicio Nacional de Sanidad, Inocuidad y Calidad Agroalimentaria (1999). Norma Oficial Mexicana NOM-062-ZOO-1999.
- Eslava, C., Navarro-García, F., Czezulín, J.R., Henderson, I.R., Cravioto, A. & Nataro, J.P. (1998). Pet, an autotransporter enterotoxin from enteroaggregative *Escherichia coli*. *Infect. Immun.*, **66**(6), 3155-3163
- Gutiérrez-Lucas, L., Mendoza-Hernández, G., González-Pedrajo, B., Eslava-Campos, C., Bustos-Martínez, J. & Sainz-Españes, T. (2012). Identification of the autotransporter Pet toxin in *Proteus mirabilis* strain isolated from patients with urinary tract infection. *Adv. Biol. Chem.*, **2**(3), 283-290. DOI: 10.4236/abc.2012.23036
- Hannan, T.J., Mysorekar, I.U., Hung, C.S., Isaacson-Schmid, M.L. & Hultgren S.J. (2010). Early severe inflammatory responses to uropathogenic *Escherichia coli* predispose to chronic and recurrent urinary tract infection. *PLoS Pathog.*, **6**, 1-19. DOI: 10.1371/journal.ppat.1001042
- Henderson, I.R., Hicks, S., Navarro-García, F., Elias, W.P., Philips, A.D. & Nataro, J.P. (1999). Involvement of the enteroaggregative *Escherichia coli* plasmid-encoded toxin in causing human intestinal damage. *Infect. Immun.*, **67**(10), 5336-5344
- Henderson, I.R., Navarro-García, F., Desvaux, M., Fernandez, R.C. & Ala'Aldeen, D. (2004). Type V protein secretion pathway the autotransporter story. *Microbiol. Mol. Biol. Rev.*, **68**(4), 692-744. DOI: 10.1128/MMBR.68.4.692-744.2004
- Herzog, K., Engeler-Dusel, J., Hugentobler, M., Beutin, L., Sägger, G., Stephan, R., Hächler, H. & Nüesch-Inderbinen, M. (2014). Diarrheagenic enteroaggregative *Escherichia*

- coli* causing urinary tract infection and bacteremia leading to sepsis. *Infection*, **42**, 441-444. DOI: doi: 10.1007/s15010-013-0569-x
- Hoeninger, J.F.M. (1964). Cellular changes accompanying the swarming of *Proteus mirabilis* I observation on living cultures. *Canadian Journal Microbiol.*, **10(1)**, 1-9. DOI: 10.1139/m64-001
- Hung, C.S., Dodson, K.W. & Hultgren, S.J. (2009). A murine model of urinary tract infection. *Nat. Protoc.*, **4(8)**, 1230-1243. DOI: 10.1038/nprot.2009.116
- Laemmli, U.K. (1970). Cleavage of structural proteins during the assembly of the head of bacteriophage T4. *Nature*, **227(5259)**, 680-685
- Mobley, H.L.T. & Belas, R. (1995). Swarming and pathogenesis of *Proteus mirabilis* in the urinary tract. *Trends Microbiol.*, **3(7)**, 280-284. DOI: 10.1016/S0966-842X(00)88945-3
- Nataro, J.P., Deng, Y., Cookson, S., Cravioto, A., Savarino, S.J., Guers, L.D., Levine, M.M. & Tacket, C.O. (1995). Heterogeneity of enteroaggregative *Escherichia coli* virulence demonstrated in volunteers. *J. Infec. Dis.*, **171(2)**, 465-468
- Navarro-García, F., Eslava, C., Villaseca, J.M., López-Revilla, R., Czczulin, J.R., Srinivas, S., Nataro, J.P. & Cravioto, A. (1998). *In vitro* effects of high-molecular-weight heat-labile enterotoxin from enteroaggregative *Escherichia coli*. *Infect. Immun.*, **66(7)**, 3149-3154.
- Navarro-García, F., Sears, C., Eslava, C., Cravioto, A. & Nataro, J.P. (1999). Cytoskeletal effects induced by Pet, the serine protease enterotoxin of enteroaggregative *Escherichia coli*. *Infect. Immun.*, **67(5)**, 2184-2192
- Navarro-García, F., Sonnested, M. & Tetter, K. (2010). Host-toxin interactions involving EspC and Pet, two serine protease autotransporters of the Enterobacteriaceae. *Toxins*, **2(5)**, 1134-1147. DOI: 10.3390/toxins2051134
- O' Hara, C. M., Branner, F.W. & Miller, J. M. (2000). Classification identification and clinical significances of *Proteus*, *Providencia* and *Morganella*. *Clin. Microbiol. Rev.*, **13(4)**, 534-546. DOI: 10.1128/CMR.13.4.534
- Reis, L.O., Sopena, J.M., Fávoro, W.J., Martin, M.C., Simão, A.F., Reis, R.B., Andrade, M.F., Domenech, J.D. & Cardo, C.C. (2011). Anatomical features of the urethra and urinary bladder catheterization in female mice and rats an essential translational tool. *Acta Cir. Bras.*, **26(2)**, 106-110. DOI: 10.1590/S0102-86502011000800019
- Rocha-Ramírez, L.M., Hernández-Chiñas, U., Baños-Rojas, D., Xicohtencatl-Cortés, J., Chávez-Berrocal, M.E., Rico-Rosillo, G., Kretschmer, R. & Eslava C.A. (2016). Pet serine protease from enteroaggregative *Escherichia coli* stimulate the inflammatory response activating human macrophages. *BMC Microbiol.*, **16(158)**, 1-10. DOI: 10.1186/s12866-016-0775-7
- Ruiz, R.C., Melo, K.C., Rossato, S.S., Barbosa, C.M., Corrêa, L.M., Elias, W.P. & Piazza, M.F. (2014). Atypical enteropathogenic *Escherichia coli* secretes Plasmid Encoded Toxin. *BioMed Res. Int.*, **20(14)**, 1-8 DOI: 10.1155/2014/896235
- Olesen, B., Scheutz, F., Andersen, R.L., Menard, M., Boisen, N., Johnston, B., Hansen, D.S., Krogfelt, K.A., Nataro, J.P. & Johnson, J.R. (2012). Enteroaggregative *Escherichia coli* O78:H10 the cause of an outbreak of urinary tract infection. *J. Clin. Microb.*, **50(11)**, 3703-3711. DOI: 10.1128/JCM.01909-12
- Sainz, T., Pérez, J., Fresan, M.C., Flores, V., Jiménez, L., Hernández, U., Herrera, I. & Eslava, C.A. (2002). Histological alterations and immune response induced by pet toxin during colonization with enteroaggregative *Escherichia coli* (EAEC) in a mouse model infection. *J. Microbiol.*, **40(2)**, 91-97
- Sui, B.Q., Dutta, P.R. & Nataro J.P. (2003). Intracellular expression of the plasmid-encoded toxin from enteroaggregative *Escherichia coli*. *Infect. Immun.*, **71(9)**, 5364-5370. DOI: 10.1128/IAI.71.9.5364-5370.2003
- Towbin, H., Staehelin, T. & Gordon, J. (1979). Electrophoretic transfer of proteins from polyacrylamide gels to nitrocellulose sheets procedure and some application. *Proc. Natl. Acad. Sci. USA.*, **76(9)**, 4350-4354
- Villaseca, J.M., Navarro-García, F., Mendoza-Hernández, G., Nataro, J.P., Cravioto, A. & Eslava, C. (2000). Pet toxin from enteroaggregative *Escherichia coli* produces cellular damage associated with fodrin disruption. *Infect. Immun.*, **268(10)**, 5920-5927